

Proton 0.01 MeV resonance width and low-energy S -factor of $p + {}^{10}\text{B}$ fusion

A. M. Mukhamedzhanov^{1,*}

¹*Cyclotron Institute, Texas A&M University, College Station, TX 77843, USA*

Background: The ${}^{10}\text{B}(p, \alpha){}^7\text{Be}$ reaction is of interest for nuclear reaction theory, nuclear astrophysics and is important for neutronless (aneutronic) fusion ${}^{11}\text{B}(p, 2\alpha){}^4\text{He}$. At low-energies the S -factor of the ${}^{10}\text{B}(p, \alpha){}^7\text{Be}$ reaction is contributed by the near-threshold resonance ($E_x = 8.70 \text{ MeV}; \frac{5}{2}^+$) with the resonance energy $E = 0.01 \text{ MeV}$ and by higher resonances. Contrary to the α -width, the proton resonance width of this resonance is unknown.

Purpose: In this paper, the proton resonance width of the near-threshold resonance is calculated using two different approaches. The values of the proton width are used to calculate the low-energy S -factor.

Method: First, the proton resonance width is estimated using the mirror symmetry of the resonance ${}^{11}\text{C}(E_x = 8.70 \text{ MeV}; \frac{5}{2}^+)$ and the mirror bound state ${}^{11}\text{B}(E_x = 9.272 \text{ MeV}; \frac{5}{2}^+)$. In the second approach, this width is estimated using the R -matrix definition of the observable resonance width, which is expressed in terms of the $p - {}^{10}\text{B}$ resonant wave function calculated in the potential approach and the spectroscopic factor.

Results: Depending on the method chosen, the calculated proton resonance width varies from $1.03 \times 10^{-19} \text{ MeV}$ to $2.96 \times 10^{-19} \text{ MeV}$. The role of the near-threshold resonance is determined using fitting of two low-energy S -factors from direct measurements [C. Angulo *et al.*, *Z. Phys. A* **345**, 333 (1993)] and from the indirect Trojan horse method (THM) [A. Cvetinović *et al.*, *Phys. Rev. C* **97**, 065801 (2018)]. Within the framework of the R -matrix method using the determined proton resonance widths and the modified THM parameters for six low-lying resonances, the low-energy S -factors were calculated and compared with the corresponding experimental S -factors. The closest agreement with the data is achieved with the proton resonance widths $1.0 \times 10^{-19} \text{ MeV}$ when fitting the S -factor from the THM indirect measurements, and $1.68 \times 10^{-19} \text{ MeV}$ and $2.5 \times 10^{-19} \text{ MeV}$ when fitting the S -factor from [Angulo *et al.*, *Z. Phys. A* **345**, 333 (1993)].

Conclusion: Our calculated proton resonance widths using the mirror symmetry and the R -matrix method are an order of magnitude larger than the phenomenological S -factor determined from the R -matrix fit of the latest measurements [Van de Kolk *et al.*, *Phys. Rev. C* **105**, 055802 (2022)]. Using the theoretically determined proton resonance widths we achieved excellent fits of the low-energy S -factors determined from the direct and indirect measurements.

I. INTRODUCTION

The ${}^{10}\text{B}(p, \alpha){}^7\text{Be}$ reaction at low energy is of interest to nuclear physics, nuclear astrophysics, and applied physics. This reaction allows nuclear physicists to investigate low-energy ${}^{11}\text{C}$ resonances at excitation energies $E_x \geq 8.70 \text{ MeV}$, which are above the proton and α decay channels. There are controversies about the location and spin-parity assignments of low-energy ${}^{11}\text{C}$ resonances. Fig. 1 depicts the low-energy resonances taken from compilation [1], from the latest R -matrix fit to the experimental cross-section of the ${}^{10}\text{B}(p, \alpha){}^7\text{Be}$ reaction and from the indirect THM [3]. One can see that the R -matrix fit to direct measurements [2] in the energy interval $E = 0.73 - 1.82 \text{ MeV}$, where $E \equiv E_{p, {}^{10}\text{B}}$ is the $p - {}^{10}\text{B}$ relative kinetic energy, required change of two resonance assignments given in compilation [1]. In particular, the level $\frac{3}{2}^+$ just above the level ($8.70 \text{ MeV}; \frac{5}{2}^+$) is quite plausible because a similar level is observed in the mirror nucleus ${}^{11}\text{B}$. However, in the recently published paper [4] within the framework of the shell model embedded in the continuum (SMEC) was confirmed the presence

of the level ($E_x = 9.20 \text{ MeV}; \frac{5}{2}^+$) rather than the level ($E_x = 9.74 \text{ MeV}; \frac{3}{2}^+$). Besides, the THM experiment [3] suggested that there is a new level, ($E_x = 9.36 \text{ MeV}; \frac{5}{2}^-$), which was not mentioned in the literature before.

This uncertainty regarding the low-level resonances in ${}^{11}\text{C}$ requires further analysis because they affect the low-energy cross-section and S -factor of the ${}^{10}\text{B}(p, \alpha){}^7\text{Be}$ reaction. It is the reason why in this paper, we constrained our fit by $E < 0.3 \text{ MeV}$, where the near-threshold resonance ($E_x = 8.70 \text{ MeV}; \frac{5}{2}^+$) dominates.

In nuclear astrophysics, the ${}^{10}\text{B}(p, \alpha){}^7\text{Be}$ reaction represents the main ${}^{10}\text{B}$ destruction channel in H-rich main-sequence outer layers of stars with the Gamow window energy $0.01 \pm 0.005 \text{ MeV}$ for such stellar environments [3]. The $\frac{5}{2}^+$ resonance at $E_R = 0.01 \text{ MeV}$ corresponding to the excitation energy $E_x = 8.70 \text{ MeV}$ of ${}^{11}\text{C}$ (see Fig. 1) dominates the ultra low-energy cross-section of the ${}^{10}\text{B}(p, \alpha){}^7\text{Be}$ reaction. This resonance is key in predicting boron abundances and constraining mixing phenomena in such stars [5].

Another role of the ${}^{10}\text{B}(p, \alpha){}^7\text{Be}$ reaction is related to neutronless (also called aneutronic synthesis [2]) laser-driven, hot-plasma fusion, which attracts increasing attention as a new energy source that would be free of radioactive products with large half-life. One of the

* akram@comp.tamu.edu

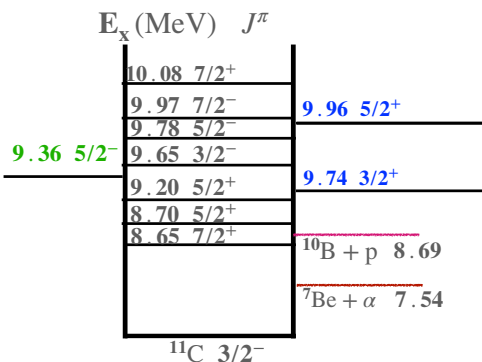


FIG. 1. The energy levels of ^{11}C contributing to low-energy $^{10}\text{B}(p, \alpha)^7\text{Be}$ reaction cross-section. E_x is the excitation energy expressed in MeV. Only levels slightly above the proton threshold and one subthreshold bound state in the channel $^{10}\text{B} + p$ are shown. The black numbers are data taken from [1]. The blue data are from the recent R -matrix fit to the S -factor and cross-section of the $^{10}\text{B}(p, \alpha)^7\text{Be}$ reaction reported in [2]. The green numbers are taken from [3]. The red lines are the proton and α -channel thresholds.

sources of the aneutronic fusion is the $^{11}\text{B}(p, 2\alpha)^4\text{He}$ ($Q = 8.7$ MeV) reaction. Natural boron contains $\sim 80\%$ of the ^{11}B isotope and $\sim 20\%$ of ^{10}B . The presence of the isotope ^{10}B results in the collateral reaction $^{10}\text{B}(p, \alpha)^7\text{Be}$ ($Q = 1.152$ MeV), which can contaminate the fusion reactors due to the generation of the radioactive ^7Be . But the $^{10}\text{B}(p, \alpha)^7\text{Be}$ reaction plays a positive role in providing an additional tool to measure the temperature of hot plasma used in ignition facilities (see [2] and references therein). Note that very low energies (~ 0.01 MeV) is the operational regime of the National Ignition Facility (NIF).

The most advanced measurements of the $^{10}\text{B}(p, \alpha)^7\text{Be}$ S -factor were reported in Refs.[6–8] and [2]. The work [6] presented the lowest direct measurements of the S -factor of the $^{10}\text{B}(p, \alpha)^7\text{Be}$ reaction. Other three papers, [3, 7, 8], addressed the indirect measurements of the S -factor in the energy region $E = 0.005 - 1.5$ MeV using the THM. It is the lowest measured energy interval; however, the uncertainty of the measured S -factor quickly increases as the energy decreases. The most accurate direct measurements of the $^{10}\text{B}(p, \alpha)^7\text{Be}$ cross-section and S -factor were recently reported in [2] in which the $^{10}\text{B}(p, \alpha)^7\text{Be}$ cross-section was measured in the proton energy interval $0.8 - 2.0$ MeV. It is an excellent work in which the uncertainties of the measured cross-section and S -factors were reduced to $\approx 10\%$ in the measured energy interval.

The very low-energy cross-section of $^{10}\text{B}(p, \alpha)^7\text{Be}$, contributed by the $E_R = 0.01$ MeV resonance, depends on the proton resonance width in the entry channel and the α -particle resonance width in the exit channel of the reaction. While the latter is well established, $\Gamma_\alpha = 0.015$ keV [1], the proton resonance width, which could be crucial for the $^{10}\text{B}(p, \alpha)^7\text{Be}$ cross-section and S -factor evalua-

tions, is the subject to large uncertainty.

In this paper, I will present a theoretical evaluation of the proton resonance width of the $E_R = 0.01$ MeV resonance using two different theoretical approaches, mirror symmetry and R -matrix, and check an impact of the proton resonance width on the low-energy S -factor of the $^{10}\text{B}(p, \alpha)^7\text{Be}$ reaction. Both methods give results by about an order of magnitude larger than the phenomenological proton resonance width obtained in [2] using the R -matrix fitting to the higher-energy experimental data. Obtained higher proton resonance widths allowed us to fit the low-energy S -factors from [6] and [3]. The paper uses the system of units in which $\hbar = c = 1$.

II. PROTON RESONANCE WIDTH FROM MIRROR SYMMETRY OF $^{11}\text{C}(E_x = 8.70$ MeV) AND $^{11}\text{B}(E_x = 9.272$ MeV)

The width of a narrow resonance can be expressed in terms of the ANC of the Gamow-Siegert wave function [9]. That is why we can extend the relationship between the ANCs of mirror bound states to the relationship between resonance widths and ANCs of the mirror nuclei [10, 11]. The calculated resonance widths and the ANCs depend strongly on the choice of the nucleon-nucleon (NN) force, but the ratios of the resonance widths and the ANCs for mirror bound states should not depend on the adopted NN force, see for details review [12].

Another important feature of the mirror nuclei is the similarity of the internal mirror wave functions. Let us consider a mirror pair in a two-body potential model: $B_1 = (a_1 A_1)$ in the resonance state and the loosely bound nucleus $B_2 = (a_2 A_2)$. The mirror resonance state is obtained by replacing one of the neutrons with a proton. The additional Coulomb interaction pushes the bound-state level into a resonance level. The resonance and binding energy of the mirror states are significantly smaller than the depth of the nuclear potential. The Coulomb interaction is almost a constant in the nuclear interior. Hence, in the nuclear interior, which is all that matters to determine the ratio of the resonance width and the ANC of the mirror state, the radial behavior of the mirror wave functions, which are both real, is very similar, and they differ only by normalization. In the outer region, the resonant and bound-state wave functions vary significantly.

In the case under consideration, we consider the resonance state $^{11}\text{C} = (p^{10}\text{B})[E_x = 8.70$ MeV; $\frac{5}{2}^+$] and the mirror bound state $^{11}\text{B} = (n^{10}\text{B})[E_x = 9.272$ MeV; $\frac{5}{2}^+$]. Following [11], we express the ratio of the resonance width $\Gamma_{(p)l_p j_p}$ of the resonance state of ^{11}C and the ANC $C_{(n)l_n j_n}$ of the mirror bound state ^{11}B [9] in terms of the ratio of the Wronskians \mathcal{W} :

$$\frac{\Gamma_{(p)l_p j_p}}{(C_{(n)l_n j_n})^2} = \sqrt{\frac{2E}{\mu_{pA}}} \frac{\left| \kappa_{nA} \mathcal{W}[I_{l_p j_p}(k_{pA}, r_{pA}), F_{l_p}(k_{pA}, r_{pA})] \right|^2 \Big|_{r_{pA}=R_{ch}}}{\left| k_{pA} \mathcal{W}[I_{l_n j_n}(\kappa_{nA}, r_{nA}), F_{l_n}(i\kappa_{nA}, r_{nA})] \right|^2 \Big|_{r_{nA}=R_{ch}}} \quad (1)$$

$$\approx \frac{S_{l_p j_p}}{S_{l_n j_n}} \sqrt{\frac{2E}{\mu_{pA}}} \frac{\left| \kappa_{nA} \mathcal{W}[\varphi_{l_p j_p}(k_{pA}, r_{pA}), F_{l_p}(k_{pA}, r_{pA})] \right|^2 \Big|_{r_{pA}=R_{ch}}}{\left| k_{pA} \mathcal{W}[\varphi_{l_n j_n}(\kappa_{nA}, r_{nA}), F_{l_n}(i\kappa_{nA}, r_{nA})] \right|^2 \Big|_{r_{nA}=R_{ch}}}. \quad (2)$$

where the ratio $\frac{\Gamma_{(p)l_p j_p}}{(C_{(n)l_n j_n})^2}$ is dimensionless, R_{ch} is the channel radius dividing the configuration space into the internal and external regions. $I_{l_p j_p}$ is the proton overlap function determining the projection of the bound-state wave function of nucleus ^{11}C on the channel $p+^{10}\text{B}$, and $I_{l_n j_n}$ is the neutron overlap function determining the projection of the bound-state wave function of nucleus ^{11}B on the channel $n+^{10}\text{B}$. l_p and j_p (l_n and j_n) are the proton (neutron) orbital angular momentum and total angular momentum in nucleus ^{11}C (^{11}B). For the case under consideration $l_p = l_n = 0$, $j_p = j_n = 1/2$. $E \equiv E_{pA}$ and μ_{pA} are the real part of the resonance energy and the reduced mass of the $p-A$ pair, which are expressed in MeV. k_{pA} is the $p-A$ relative momentum and κ_{nA} is the bound-state wave number of the bound state (nA), $F_{l_p}(k_{pA}, r_{pA})$ is the regular Coulomb solution of the $p+$

A scattering. $F_{l_n}(i\kappa_{nA}, r_{nA})$ is the regular solution of the free $n+A$ scattering.

To obtain Eq. (2) we use the single-particle approximation in the internal region

$$I_{l_n j_n}(r_{nA}) = S_{l_n j_n}^{1/2} \varphi_{l_n j_n}(r_{nA}). \quad (3)$$

Since the the Wronskian ratio (1) is taken at the channel radius, we can use the proton resonance wave $\varphi_{l_p j_p}$ and the mirror neutron bound-state wave function $\varphi_{l_n j_n}$, which are normalized to the unity over the internal region ($r_{pA} \leq R_{ch}$ and $r_{nA} \leq R_{ch}$). $S_{l_n j_n}$ is the single-particle spectroscopic factor (SF) of the $(N-A)_{l_n j_n}$.

If the SFs of the mirror states are the same,

$$S_{l_p j_p} = S_{l_n j_n}, \quad (4)$$

then Eq. (2) reduces to

$$\frac{\Gamma_{(p)l_p j_p}}{(C_{(n)l_n j_n})^2} \approx \sqrt{\frac{2E}{\mu_{pA}}} \frac{\left| \kappa_{nA} \mathcal{W}[\varphi_{l_p j_p}(k_{pA}, r_{pA}), F_{l_p}(k_{pA}, r_{pA})] \right|^2 \Big|_{r_{pA}=R_{ch}}}{\left| k_{pA} \mathcal{W}[\varphi_{l_n j_n}(\kappa_{nA}, r_{nA}), F_{l_n}(i\kappa_{nA}, r_{nA})] \right|^2 \Big|_{r_{nA}=R_{ch}}}. \quad (5)$$

Equations (1), (2) and (5) allow one to determine the resonance width if the ANC of the mirror bound state is known and vice versa. The mirror wave functions, $\varphi_{l_p j_p}(k_{pA}, r_{pA})$ and $\varphi_{l_n j_n}(\kappa_{nA}, r_{nA})$, are calculated using similar two-body $N-A$ nuclear potentials. In the internal region ($r \leq R_{ch}$), which is needed to calculate the right-hand-side of Eqs. (2) and (5), both wave functions are real and their radial behavior, due to the mirror symmetry, should look very similar.

We can further simplify Eq. (5). The Coulomb interaction varies very little in the nuclear interior, and its effect only leads to shifting the bound state's energy to the

continuum. Hence, it can be assumed that $F_{l_p}(k_{pA}, r_{pA})$ and $F_{l_n}(i\kappa_{nA}, r_{nA})$ behave similarly in the nuclear interior except for the overall normalization, that is,

$$F_{l_p}(k_{pA}, r_{pA}) \approx \frac{F_{l_p}(k_{pA}, R_{ch})}{F_{l_n}(i\kappa_{nA}, R_{ch})} F_{l_n}(i\kappa_{nA}, r_{nA}). \quad (6)$$

Neglecting further the difference between the mirror wave functions $\varphi_{l_p j_p}(k_{pA}, r_{pA})$ and $\varphi_{l_n j_n}(\kappa_{nA}, r_{nA})$ in the nuclear interior we obtain the approximate expression

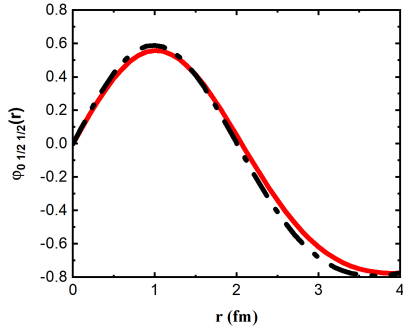


FIG. 2. Internal single-particle resonance (solid red line) and bound-state (black dash-dotted line) wave functions of $^{11}\text{C}(E_x = 8.70 \text{ MeV}; \frac{5}{2}^+)$ and $^{11}\text{B}(E_x = 9.272 \text{ MeV}; \frac{5}{2}^+)$ states, respectively. Both wave functions are normalized to unity in the internal region $0 \leq r \leq 4 \text{ fm}$.

for $\frac{\Gamma_{(p)l_p j_p}}{(C_{(n)l_n j_n})^2}$:

$$\frac{\Gamma_{(p)l_p j_p}}{(C_{(n)l_n j_n})^2} \approx \sqrt{\frac{2E}{\mu_{pA}}} \left| \frac{F_{l_p}(k_{pA}, R_{ch})}{F_{l_n}(i\kappa_{nA}, R_{ch})} \right|^2. \quad (7)$$

This equation provides the easiest way to determine $\frac{\Gamma_{(p)l_p j_p}}{(C_{(n)l_n j_n})^2}$ because to calculate it one needs to know only the Coulomb scattering wave function in continuum and free scattering wave function at imaginary momentum for the mirror bound state. However, Eq. (7) is less accurate than Eq. (2).

Figs. 2 and 3 show resonance and bound-state wave functions normalized in the internal regions $0 \leq r \leq 4 \text{ fm}$ and $0 \leq r \leq 5 \text{ fm}$, respectively. The single-particle resonance and bound-state wave functions presented in

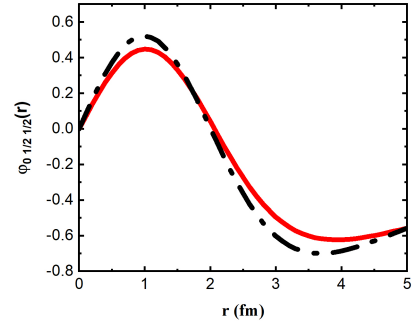


FIG. 3. The same as in Fig. 2 but for $0 \leq r \leq 5 \text{ fm}$.

these figures are calculated using the Woods-Saxon potential with the radial parameter $r_0 = 1.27 \text{ fm}$ and diffuseness $a = 0.67 \text{ fm}$ [4]. The depth of the potential is $V_0 = 61.7065 \text{ MeV}$ for the resonance state, and $V_0 = 63.0952 \text{ MeV}$ for the mirror bound state. Since the nucleon orbital angular momentum in the mirror states $^{11}\text{C} = (p^{10}\text{B})[E_x = 8.70 \text{ MeV}; \frac{5}{2}^+]$ and $^{11}\text{B} = (n^{10}\text{B})[E_x = 9.272 \text{ MeV}; \frac{5}{2}^+]$ is $l_N = 0$, spin-orbital interaction vanishes. We inspect that the normalized in the internal regions mirror wave functions with $R_{ch} = 4, 5 \text{ fm}$ are very close reflecting mirror symmetry property ².

² The resonance and bound-state wave functions are normalized to unity and compared only in the internal region, where the resonance wave function is a real function and can be compared with the bound-state one. The R -matrix method employs such normalized resonant wave functions to determine the resonance width.

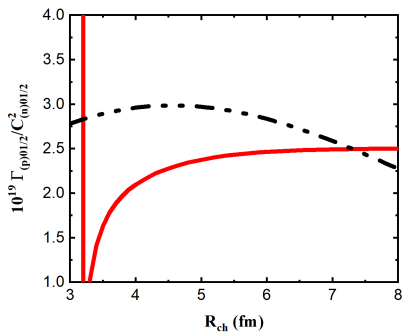


FIG. 4. Ratio $\frac{\Gamma_{(p)0\frac{1}{2}}}{(C_{(n)0\frac{1}{2}})^2}$ determined from mirror symmetry of $^{11}\text{C}(E_x = 8.70 \text{ MeV}; \frac{5}{2}^+)$ and $^{11}\text{B}(E_x = 9.27 \text{ MeV}; \frac{5}{2}^+)$ states. The solid red line is determined using Eq. (5), and the black dash-dotted-dotted line is determined using Eq. (7). Note that a discontinuity of the solid red line is caused by the node of the bound-state wave function at $r \approx 2 \text{ fm}$, see Figs. 2 and 3.

Fig. 4 shows the ratio $\frac{\Gamma_{(p)0\frac{1}{2}}}{(C_{(n)0\frac{1}{2}})^2}$ determined from Eqs. (5) and (7). From Eq. (5) we get $\frac{\Gamma_{(p)0\frac{1}{2}}}{(C_{(n)0\frac{1}{2}})^2} = 1.5 \times 10^{-19} \text{ MeVfm}$ for $R_{ch} = 4$ and 5 fm. Less accurate value is determined from Eq. (7): $\frac{\Gamma_{(p)0\frac{1}{2}}}{(C_{(n)0\frac{1}{2}})^2} = 2.4 \times 10^{-19} \text{ MeVfm}$ at $R_{ch} = 4.6 \text{ fm}$ corresponding to the peak of the ratio $\frac{\Gamma_{(p)0\frac{1}{2}}}{(C_{(n)0\frac{1}{2}})^2}$.

To determine the proton resonance width, we need the neutron ANC for the virtual breakup $^{11}\text{B}[E_x = 9.27 \text{ MeV}; \frac{5}{2}^+] \rightarrow n + ^{10}\text{B}$.

1. Shell-model ANC of neutron removal from $^{11}\text{B}[E_x = 9.27 \text{ MeV}; \frac{5}{2}^+]$

One can get this ANC by multiplying the single-particle ANC by the square root of the neutron's SF. However, the SF is not an observable quantity [13, 14] and depends on the method and model used to determine it.

First, we use the SF determined from the shell model and the single-particle potential from [4]. The single-particle neutron ANC is determined as the amplitude of the tail of the neutron bound-state wave function normalized to unity in the entire coordinate space [12]. This wave function is calculated in the above-presented Woods-Saxon potential. The estimated in [4] the proton's SF of the resonance state $^{11}\text{C} = (p^{10}\text{B})[E_x = 8.70 \text{ MeV}; \frac{5}{2}^+]$ is 0.33, which is close to the phenomenological SF $S_p = 0.31$ determined in [2] from the R -matrix fitting to the low-energy experimental data. Owing to the mirror symmetry of the resonance state $(p^{10}\text{B})[E_x = 8.70 \text{ MeV}; \frac{5}{2}^+]$ and the bound

state $(n^{10}\text{B})[E_x = 9.27 \text{ MeV}; \frac{5}{2}^+]$ I assume the same SF for both states. Then the ANC for the virtual breakup $^{11}\text{B}[E_x = 9.27 \text{ MeV}; \frac{5}{2}^+] \rightarrow n + ^{10}\text{B}$ is $C_n = 1.114 \text{ fm}^{-1/2}$. Using this ANC, we find from Eqs. (5) and (7) $\Gamma_{(p)0\frac{1}{2}} = 1.87 \times 10^{-19} \text{ MeV}$ for $R_{ch} = 4.0$ and 5.0 fm and less accurate $\Gamma_{(p)0\frac{1}{2}} = 2.96 \times 10^{-19} \text{ MeV}$ for $R_{ch} = 4.6 \text{ fm}$, respectively.

2. ANC of of neutron removal from $^{11}\text{B}[E_x = 9.27 \text{ MeV}; \frac{5}{2}^+]$ from stripping reactions

In Refs. [15] and [16] the nucleon stripping reactions $^{10}\text{B}(^3\text{He}, d)^{11}\text{C}$ and $^{10}\text{B}(d, p)^{11}\text{B}$ were studied at low energies. The differential cross sections of the reactions populating 8.65 – 8.69 MeV and 9.19 – 9.27 MeV doublets in ^{11}C and ^{11}B were measured. The determined SFs of the mirror 8.69 MeV in ^{11}C and 9.27 MeV in ^{11}B are 0.2 and 0.17, respectively. For the neutron bound-state potential parameters in ^{11}B the single-particle ANC is $2.0 \text{ fm}^{-1/2}$. Then the ANC from the $^{10}\text{B}(d, p)^{11}\text{B}$ is $0.83 \text{ fm}^{-1/2}$. Since the proton SF of the ^{11}C is slightly higher than the neutron one to determine the resonance width, we are supposed to use Eq. (2). However, there is no explanation in Ref. [15] how transfer to resonance was calculated and how the resonance wave function was normalized. That is why I still assume the SFs for the mirror states under consideration are the same.

Taking into account that from Eq. (5) we get $\frac{\Gamma_{(p)0\frac{1}{2}}}{(C_{(n)0\frac{1}{2}})^2} = 1.5 \times 10^{-19} \text{ MeVfm}$ for $R_{ch} = 4$ and 5 fm and that the neutron ANC from the $^{10}\text{B}(d, p)^{11}\text{B}$ reaction is $0.83 \text{ fm}^{-1/2}$ we get $\Gamma_{(p)0\frac{1}{2}} = 1.03 \times 10^{-19} \text{ MeV}$ for $R_{ch} = 4$ and 5 fm.

Less accurate value of the ratio $\frac{\Gamma_{(p)0\frac{1}{2}}}{(C_{(n)0\frac{1}{2}})^2} = 2.4 \times 10^{-19} \text{ MeVfm}$ at $R_{ch} = 4.6 \text{ fm}$ obtained from Eq. (7) and the proton ANC $0.83 \text{ fm}^{-1/2}$ lead to $\Gamma_{(p)0\frac{1}{2}} = 1.65 \times 10^{-19} \text{ MeV}$.

III. PROTON RESONANCE WIDTH OF RESONANCE AT $E_R = 0.01 \text{ MeV}$ FROM R-MATRIX APPROACH

In the R -matrix method the observable proton resonance width is determined by

$$\Gamma_{(p)0\frac{1}{2}} = 2 P_0(E_R, R_{ch}) \gamma_{(p)0\frac{1}{2}}^2. \quad (8)$$

² Contemporary value of the excitation energy of this level is 8.70 MeV.

Here $P_0(E_R, R_{ch})$ is the penetrability factor in the $l_p = 0$ partial wave,

$$\gamma_{(p)0\frac{1}{2}}^2 = \mathbf{S}_{(p)0\frac{1}{2}} \frac{\tilde{\gamma}_{(p)0\frac{1}{2}}^2}{1 + \tilde{\gamma}_{(p)0\frac{1}{2}}^2 \left. \frac{d\hat{S}_0(E)}{dE} \right|_{E=E_R}} \quad (9)$$

is the observable reduced width of the resonance state (see Appendix), $\hat{S}_0(E)$ is the R -matrix shift factor in the $l_p = 0$ partial wave.

$$\tilde{\gamma}_{(p)0\frac{1}{2}}^2 = \frac{\varphi_{0\frac{1}{2}}^2(R_{ch})}{2\mu_{pA} R_{ch}} \quad (10)$$

is the formal R -matrix reduced width, $\varphi_{0\frac{1}{2}}(r_{pA})$ is the internal resonance radial wave function normalized to unity in the internal region $0 \leq r \leq R_{ch}$. For $R_{ch} = 4.0$ fm we get $\varphi_{0\frac{1}{2}}(4.0 \text{ fm}) = -0.775 \text{ fm}^{-1/2}$, $\tilde{\gamma}_{0\frac{1}{2}} = -1.851 \text{ MeV}^{1/2}$. For the proton SF $\mathbf{S} = 0.31$ we get $\gamma_{(p)0\frac{1}{2}} = -0.64 \text{ MeV}^{1/2}$. The penetrability factor $P_0(0.01 \text{ MeV}, 4.0 \text{ fm}) = 2.05 \times 10^{-19}$ and $\Gamma_{(p)0\frac{1}{2}} = 1.683 \times 10^{-19} \text{ MeV}$.

For $R_{ch} = 5.0$ fm we get $\varphi_{0\frac{1}{2}}(5.0 \text{ fm}) = -0.557 \text{ fm}^{-1/2}$, $\tilde{\gamma}_{0\frac{1}{2}} = -1.190 \text{ MeV}^{1/2}$ and $\gamma_{(p)0\frac{1}{2}} = -0.483 \text{ MeV}^{1/2}$. The penetrability factor $P_0(0.01 \text{ MeV}, 5.0 \text{ fm}) = 3.99 \times 10^{-19}$ and $\Gamma_{(p)0\frac{1}{2}} = 1.863 \times 10^{-19} \text{ MeV}$.

IV. DISCUSSION OF THE OBTAINED PROTON RESONANCE WIDTH

The summary of the obtained in this paper theoretical proton resonance widths of the near-threshold resonance $^{11}\text{C} = (p^{10}\text{B})[E_x = 8.70 \text{ MeV}; \frac{5}{2}^+]$ using the mirror symmetry and the R -matrix approach are presented

V. ASTROPHYSICAL S -FACTOR FOR ^{10}B -PROTON FUSION REACTION

In this section the results of calculations of the S -factor for the low-energy $^{10}\text{B}(p, \alpha)^7\text{Be}$ reaction are presented. We consider the energy region where the contribution from the near-threshold resonance at $E_R = 0.01$ MeV dominates. Fitting to available low-energy data will allow us to determine the proton resonance width $\Gamma_{(p)0\frac{1}{2}}$.

We use the proton resonance widths $\Gamma_{(p)0\frac{1}{2}}$ determined from mirror symmetry and R -matrix method. Since we consider only very low energies, we took into account the contributions from the near-threshold resonance at $(8.70 \text{ MeV}; \frac{5}{2}^+)$ and the resonance $(9.20 \text{ MeV}; \frac{5}{2}^+)$, which interferes with the near-

threshold resonance. The results vary by a factor of three. However, the highest value of the proton resonance width, $2.96 \times 10^{-19} \text{ MeV}$, was obtained using Eq. (7), which is less accurate than the value of $1.87 \times 10^{-19} \text{ MeV}$ obtained using Eq. (5). However, this lower value of the proton resonance width is in an excellent agreement with the results obtained using the R -matrix approach.

Note that we used two neutron ANCs. The higher one, $C_{(n)0\frac{1}{2}} = 1.114 \text{ fm}^{-1/2}$, was obtained using the SF obtained phenomenologically and from the shell-model calculations [2, 4], and the single-particle potential. The lower value of the ANC, $C_{(n)0\frac{1}{2}} = 0.83 \text{ fm}^{-1/2}$, was obtained from the $^{10}\text{B}(d, p)^{11}\text{B}(8.70 \text{ MeV}; \frac{5}{2}^+)$ reaction [15, 16]. When using mirror symmetry method we assumed that the proton SF is equal to the neutron one. The smallest proton resonance width is obtained when we assume that the proton SF is equal to the neutron one deduced from the deuteron stripping reaction.

All the calculated proton resonance widths are of the order of 10^{-19} MeV , in contrast to the phenomenological value $\Gamma_{(p)0\frac{1}{2}} = 2.3 \times 10^{-20} \text{ MeV}$ deduced in [2]. Note that a comprehensive fit was performed in [2] for higher energy data, $0.73 \leq E \leq 1.82 \text{ MeV}$. Hence extracted in [2], the proton resonance width of the near-threshold resonance $E_x = 8.70 \text{ MeV}$ was found from the extrapolation of direct measurements to the low-energy region where direct data are unavailable. The difference between the proton resonance width calculated here and the phenomenological value deduced in [2] is distinct. The SMEC approach resulted in $\Gamma_{(p)0\frac{1}{2}} = 2.2 \times 10^{-17} \text{ MeV}$ [4], which is two orders of magnitude larger than our estimations and three orders of magnitude larger than the value obtained in [2].

threshold resonance. We also took into account the subthreshold bound state (aka subthreshold resonance) $(8.65 \text{ MeV}; \frac{7}{2}^+)$ corresponding to the $(p^{10}\text{B})$ binding energy $\varepsilon = 0.04 \text{ MeV}$. To extend our calculations up to $E = 0.27 \text{ MeV}$ following [3] we included four negative parity resonances $(9.36 \text{ MeV}; \frac{5}{2}^-)$, $(9.645 \text{ MeV}; \frac{3}{2}^-)$, $(9.83 \text{ MeV}; \frac{5}{2}^-)$ and $(9.97 \text{ MeV}; \frac{7}{2}^-)$, which do not interfere with the near-threshold resonance.

A. Fitting to S -factor obtained from direct measurements

We begin with the R -matrix fitting to the S -factor from [6]. The main goal of our fit is to find the pro-

TABLE I. Proton resonance width of the near-threshold resonance (8.70 MeV; $\frac{5}{2}^+$)

Equations	Mirror symmetry	R_{ch} (fm)
	$C_{(n)0\frac{1}{2}} = 1.114 \text{ fm}^{-1/2}$	
	$\Gamma_{(p)0\frac{1}{2}}$ (MeV)	
(5)	1.87×10^{-19}	4.0 and 5.0
(7)	2.96×10^{-19}	4.6
	$C_{(n)0\frac{1}{2}} = 0.83 \text{ fm}^{-1/2}$	
	$\Gamma_{(p)0\frac{1}{2}}$ (MeV)	
(5)	1.03×10^{-19}	4.0 and 5.0
(7)	1.65×10^{-19}	4.6
	<i>R</i> -matrix approach	
	$\Gamma_{(p)0\frac{1}{2}}$ (MeV)	
(8)	1.68×10^{-19}	4.0
(8)	1.86×10^{-19}	5.0

ton resonance width of the near-threshold resonance (8.70 MeV; $\frac{5}{2}^+$), which provides the best fit to the experimental data from [6] in the low-energy region where this resonance dominates.

When considering two interfering resonances, (8.70 MeV; $\frac{5}{2}^+$) and (9.20 MeV; $\frac{5}{2}^+$), we followed the procedure described in [17]. The resonance energy of the former is taken to be equal to the first *R*-matrix energy eigenvalue and was used for the boundary condition energy, while the second *R*-matrix energy level was varied to achieve the best fit. This procedure was explained in Appendix B. The second resonance determined from the search deviates from the experimental one. After that, using Barker's transformation [17], we can find the parameters of the second resonance.

Fig. 5 depicts the low-energy *S*-factor for the $^{10}\text{B}(p, \alpha)^7\text{Be}$ reaction from [6] compared with the present work calculations. For comparison are also shown the THM experimental *S*-factor and the *S*-factor calculated using the proton resonance $\Gamma_{(p)0\frac{1}{2}} = 2.2 \times 10^{-17}$ MeV from [4]. The low-energy THM *S*-factor at $E < 0.034$ MeV becomes noticeably lower than the one from [6]. The *S*-factor calculated with the proton resonance width from [4] reveals irreconcilable difference with other *S*-factors.

We find that the best fits to the *S*-factor from [6] can be achieved using two different proton resonance widths of the resonance (8.70 MeV; $\frac{5}{2}^+$) (see Table I): $\Gamma_{(p)0\frac{1}{2}} = 1.68 \times 10^{-19}$ MeV and $\Gamma_{(p)0\frac{1}{2}} = 2.5 \times 10^{-19}$ MeV. These are the marginal values. Any resonance width between these two marginal values will provide a similar fit.

The *R*-matrix parameters of our fits to the *S*-factor from [6] are given in Table II. Note that these parameters are taken from [3] with some modifications to achieve

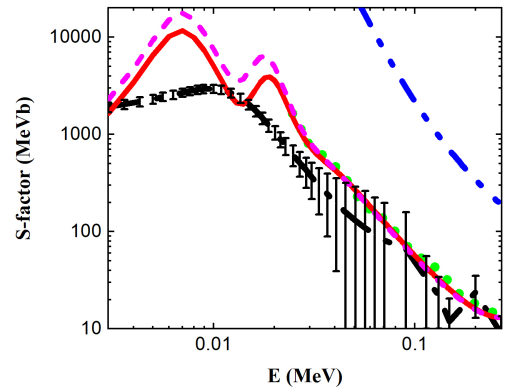


FIG. 5. Low-energy *S*-factors for the $^{10}\text{B}(p, \alpha)^7\text{Be}$ reaction. The green short dots- *S*-factor from [6]. The black dash-dotted line with errors is the THM *S*-factor [3]. The solid red (magenta dash) line is the present work best fit to data from [6] for the proton resonance width $\Gamma_{(p)0\frac{1}{2}} = 1.68 \times 10^{-19}$ MeV ($\Gamma_{(p)0\frac{1}{2}} = 2.5 \times 10^{-19}$ MeV) of the resonance $E_R = 0.01$ MeV. The blue dash-dotted-dotted line is obtained with the proton resonance width 2.2×10^{-17} MeV [4].

the best fit. In particular, the proton and α -particle resonance widths of the resonance ($E_x = 9.36$ MeV; $\frac{5}{2}^-$) are varied in our fit. Only six first resonances and one sub-threshold resonance are taken into account. The channel radius in the proton channel $R_{ch(p)} = 4.0$ fm and in the α -channel $R_{ch(\alpha)} = 4.49$ fm are employed in these calcu-

lations.

TABLE II. The parameters of the R -matrix fit corresponding to the red solid line in Fig. 5

E_x MeV	E_R MeV	J^π	l_p	l_α	$\Gamma_{(p)l_p j_p}$ MeV	$\Gamma_{(\alpha)l_\alpha j_\alpha}$ MeV
8.654	-0.354	$\frac{7}{2}^+$	2	3	2.05×10^{-27}	0.005
8.70	0.01	$\frac{5}{2}^+$	0	1	1.68×10^{-19} [2.5×10^{-19}]	0.015
9.36	0.671	$\frac{5}{2}^-$	1	2	0.085 [0.090]	0.350
9.645	0.956	$\frac{3}{2}^-$	1	0	0.048	0.223
9.83	1.140	$\frac{5}{2}^-$	1	2	0.012	0.165
9.97	1.284	$\frac{7}{2}^-$	1	2	0.221	0.066
12.98 [13.693]	4.29 [5.00]	$\frac{5}{2}^+$	0	1	0.114 [0.1303]	0.018 [0.015]

In Table II all the numbers in the brackets correspond to the resonance width $\Gamma_{(p)0\frac{1}{2}} = 2.5 \times 10^{-19}$ MeV. As explained above, in the R -matrix fit with two interfering resonances and fixed one of them, namely, the resonance (8.70 MeV; $\frac{5}{2}^+$), the second resonance (9.20 MeV; $\frac{5}{2}^+$) is replaced with the resonance which is varied. The obtained eigenenergy for the second level is $E_2 = -0.115$ MeV, which is the same for both widths $\Gamma_{(p)0\frac{1}{2}}$ listed in Table II. After applying the Barker's procedure [17] the second resonances are 4.290 MeV for $\Gamma_{(p)0\frac{1}{2}} = 1.68 \times 10^{-19}$ MeV and 5.00 MeV for $\Gamma_{(p)0\frac{1}{2}} = 2.5 \times 10^{-19}$ MeV. They are given in the last row of Table II. These resonances significantly deviate from the experimental resonance at 0.51 MeV. It means that there is a significant contribution from the $\frac{5}{2}^+$ background resonance, which was not explicitly included at the beginning but revealed itself through the fit. Since initially we took into account only two $\frac{5}{2}^+$ resonances, the effective second resonance plays the role of the background one with the proton and alpha-particle partial resonance widths given in Table II. More sophisticated fit should take into account three interfering $\frac{5}{2}^+$ resonances: 8.70, 9.20 MeV and the background resonance. An important contribution at higher energies (in our fitted energy interval) gives the resonance (9.36 MeV; $\frac{5}{2}^-$) discovered in [3], which was not listed in compilation [1]. Our S -factors at $E_R = 0.01$ MeV correspond to the cross sections: $\sigma(0.01) = 1.38 \times 10^{-12}$ mb for $\Gamma_{(p)0\frac{1}{2}} = 1.68 \times 10^{-19}$ MeV and $\sigma(0.01) = 2.05 \times 10^{-12}$ mb for $\Gamma_{(p)0\frac{1}{2}} = 2.5 \times 10^{-19}$ MeV.

The lowest measured energy 0.0246 MeV in [6] is higher than the near-threshold resonance 0.01 MeV. It is also the NIF operational energy. However, from Fig. 5 follows that the S -factor is sensitive to the variation of the proton resonance width $\Gamma_{(p)0\frac{1}{2}}$ only at energies $E < 0.021$ MeV. That is why the analysis of the data from [6] allowed us

to identify a broad range of the proton resonance widths rather than a unique value.

Only the indirect THM reached energies close to 0.01 MeV. In the next subsection, we present the results of the fitting to the THM S -factor [3].

B. Fitting THM data

There were a few publications in which THM measurements of the low-energy S -factor for the $^{10}\text{B}(p, \alpha)^7\text{Be}$ fusion were reported [3, 7, 8]. In this fit, we use the data from [3]. The fit is similar to the one described in subsection V A. The result of the fit is shown in Fig. 6. Since the THM S -factor is lower than the one from [6], we are able to determine the proton resonance width $\Gamma_{(p)0\frac{1}{2}} = 1.0 \times 10^{-19}$ MeV providing the best fit. This width is smaller than the proton resonance width interval deduced from the fit of the S -factor to data from [6]. Our S -factor perfectly fits the experimental THM one. In particular, our fit confirms the bending of the S -factor at energies below the near-threshold resonance 0.01 MeV. The behavior of the THM S -factor significantly deviates from the fit to data from [6] extrapolated down to energies $E < 0.021$ MeV.

The R -matrix amplitude has two $\frac{5}{2}^+$ interfering resonances, 8.70 and 9.20 MeV. Again, as we did for fitting the S -factor from [6], we fix the former and vary the energy of the second resonance. The R -matrix parameters of the fit to the THM S -factor from [8] are given in Table III.

The channel radii are $R_{ch(p)} = 4.0$ fm and $R_{ch(\alpha)} = 4.05$ fm. As the result of the fit, the second resonance 9.20 MeV is replaced with the resonance level 9.86 MeV. This resonance takes into account both 9.20 MeV resonance and the background one. It is worth mentioning that the resonance at 9.36 MeV is important for fitting

TABLE III. The parameters of the R -matrix fit shown as the red solid line in Fig. 6

E_x MeV	E_R MeV	J^π	l_p	l_α	$\Gamma_{(p)l_p j_p}$ MeV	$\Gamma_{(\alpha)l_\alpha j_\alpha}$ MeV
8.654	-0.354	$\frac{7}{2}^+$	2	3	2.05×10^{-27}	0.005
8.70	0.01	$\frac{5}{2}^+$	0	1	1.00×10^{-19}	0.015
9.36	0.671	$\frac{5}{2}^-$	1	2	0.05	0.450
9.645	0.956	$\frac{3}{2}^-$	1	0	0.048	0.230
9.83	1.140	$\frac{5}{2}^-$	1	2	0.012	0.165
9.86	1.17	$\frac{5}{2}^+$	0	1	0.004	0.239
9.97	1.284	$\frac{1}{2}^-$	1	2	0.221	0.066

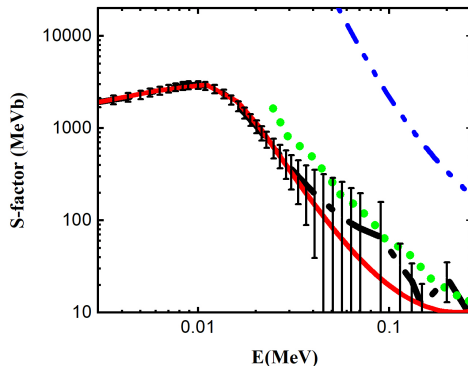


FIG. 6. The low-energy S -factors for the $^{10}\text{B}(p, \alpha)^7\text{Be}$ reaction. All the notations are the same as in Fig. 5 except for the solid red line, which is now our R -matrix fit to the THM data from [3].

at energies close to 0.27 MeV.

Our S -factor at $E_R = 0.01$ MeV corresponds to the cross-section for the $^{10}\text{B}(p, \alpha)^7\text{Be}$ reaction: $\sigma(0.01) = 1.38 \times 10^{-12}$ mb for $\Gamma_{(p)0\frac{1}{2}} = 1.0 \times 10^{-19}$ MeV.

VI. CONCLUSION

The extra low-energy $^{10}\text{B}(p, \alpha)^7\text{Be}$ reaction is dominated by the near-threshold resonance at (8.70 MeV; $\frac{5}{2}^+$). The cross-section of this reaction is defined by the proton resonance width $\Gamma_{(p)0\frac{1}{2}}$ in

the entry channel and by the α -channel resonance width in the exit channel. The latter is well established, while the former is unknown due to its smallness. This paper presents two methods of estimating the proton resonance width: mirror symmetry and R -matrix. The first one gave four different values in the interval $(1.03 - 2.5) \times 10^{-19}$ MeV, while the application of the second method resulted in $\Gamma_{(p)0\frac{1}{2}} = 1.68 \times 10^{-19}$ and 1.86×10^{-19} MeV. These widths are almost an order of magnitude larger than the phenomenological width deduced in [2], but two orders of magnitude smaller than the width from [4].

Using the found proton widths, we achieved excellent agreements with experimental low-energy S factors from [6] and [3] in the energy interval $0.001 < E < 2.7$ MeV. An important contribution to the S -factor at energies near 2.7 MeV gives the negative parity resonance at (9.36 MeV; $\frac{5}{2}^-$) MeV found in [3]. Since the lowest measured energy in [6] was 0.0246, which is higher than the near-threshold resonance 0.01 MeV, we were able to identify the interval of the resonance widths providing the best fit rather than a unique value: $\Gamma_{(p)0\frac{1}{2}} = (1.68 - 2.5) \times 10^{-19}$ MeV. The THM experiment [3] reached 0.01 Me and we were able to determine a unique value of the proton resonance width: $\Gamma_{(p)0\frac{1}{2}} = 1.0 \times 10^{-19}$ MeV.

From the fits we find the cross-sections for the $^{10}\text{B}(p, \alpha)^7\text{Be}$ reaction at $E = 0.01$ MeV: $\sigma(0.01) = 1.38 \times 10^{-12}$ mb for $\Gamma_{(p)0\frac{1}{2}} = 1.68 \times 10^{-19}$ MeV, $\sigma(0.01) = 2.05 \times 10^{-12}$ mb for $\Gamma_{(p)0\frac{1}{2}} = 2.5 \times 10^{-19}$ MeV (fits to the S -factor [6]) and $\sigma(0.01) = 1.38 \times 10^{-12}$ mb for $\Gamma_{(p)0\frac{1}{2}} = 1.0 \times 10^{-19}$ MeV (fit to the THM S -factor [3]). These values can help to determine whether the $^{10}\text{B}(p, \alpha)^7\text{Be}$ reaction is a spoiler for the $^{11}\text{B}(p, 2\alpha)^4\text{He}$ reaction used by NIF for the energy production.

The higher-energy S factor was not calculated because of the uncertainties in the location and spin-parity assignments of low-energy resonances [2, 3]. It calls for further investigation of low-energy resonances in ^{11}C .

ACKNOWLEDGMENTS

The author acknowledges that this material is based upon work supported by the US DOE National Nuclear Security Administration, under Award Number DE-NA0003841 and DOE Grant No. DE-FG02-93ER40773. The author thanks Michael Wiescher and Richard de Boer for useful discussions. The author expresses his gratitude to Arkadi Zhanov for technical support.

VII. APPENDIX

Appendix A: Internal resonance wave function in the R -matrix approach

We start from Eq. (107) [9] generalizing it for resonance states. Below we use simplified notations leaving only l -dependence of the wave functions. The resonance state can be Gamow-Siegert resonance wave function. For narrow resonance the imaginary part of the resonance energy can be neglected and the internal Gamow-Siegert wave function becomes a real, regular solution in the nuclear interior with outgoing wave O_l . Introducing Zel'dovich regulator $\lim_{\beta \rightarrow 0} e^{-\beta r^2}$ one can regularize the Gamow-Siegert wave function. Hence we can assume that the integral

$$J_0^\infty = \int_0^\infty dr \phi_l^2(k, r) \quad (\text{A.1})$$

is finite.

Then Eq. (107) [9] becomes valid for the resonance state

$$\begin{aligned} J_0^\infty &= \int_0^\infty dr \phi_l^2(k, r) = \left[1 + \int_{R_{ch}}^\infty dr \varphi_l^2(k, r) \right] \int_0^{R_{ch}} dr \phi_l^2(k, r) \\ &= \left[1 + (\tilde{\gamma}_l^{sp})^2 \frac{\partial \hat{S}(E)}{\partial E} \right] \int_0^{R_{ch}} dr \phi_l^2(k, r). \end{aligned} \quad (\text{A.2})$$

Here

$$\varphi_l(k, r) = \frac{\phi_l(k, r)}{\left[\int_0^{R_{ch}} dr \phi_l^2(k, r) \right]^{1/2}} \quad (\text{A.3})$$

is the resonant wave function normalized to unity over the internal region ($r \leq R_{ch}$), that is,

$$\int_0^{R_{ch}} dr \varphi_l^2(k, r) = 1. \quad (\text{A.4})$$

The boundary condition is

$$\begin{aligned} R_{ch} \frac{d \ln(\phi_l(k, r))}{dr} \Big|_{r=R_{ch}} &= R_{ch} \frac{d \ln(O_l(k, r))}{dr} \Big|_{r=R_{ch}} \\ &= \hat{S}(E), \end{aligned} \quad (\text{A.5})$$

where $\hat{S}(E)$ is the energy shift function. The condition (A.5) in which the wave function in the external region is giving by the outgoing wave assumes that $k = k_0$, where k_0 is the real part of the resonance momentum related to the real part of the resonance energy as $E_R = k_0^2/(2\mu)$. Hence in what follows to underscore explicitly that we deal with the resonance state, we replace k with k_0 . Assume that $\phi_l(k_0, r)$ is normalized to unity over the entire configuration space. Then

$$\begin{aligned} \phi_l^2(k_0, r) &= \frac{\varphi_l^2(k_0, r)}{1 + (\tilde{\gamma}_l^{sp})^2 \frac{\partial \hat{S}}{\partial E} \Big|_{E=E_R}} \\ &= 2\mu R_{ch} \frac{(\tilde{\gamma}_l^{sp})^2}{1 + (\tilde{\gamma}_l^{sp})^2 \frac{\partial \hat{S}}{\partial E} \Big|_{E=E_R}} \end{aligned} \quad (\text{A.6})$$

with

$$\varphi_l^2(k_0, R_{ch}) = 2\mu R_{ch} (\tilde{\gamma}_l^{sp})^2. \quad (\text{A.7})$$

$(\tilde{\gamma}_l^{sp})^2$ is the formal R -matrix single-particle reduced width and

$$(\gamma_l^{sp})^2 = \frac{(\tilde{\gamma}_l^{sp})^2}{1 + (\tilde{\gamma}_l^{sp})^2 \frac{\partial \hat{S}}{\partial E} \Big|_{E=E_R}} \quad (\text{A.8})$$

is the observable single-particle reduced width. Then

$$\phi_l^2(k_0, R_{ch}) = 2\mu R_{ch} (\gamma_l^{sp})^2. \quad (\text{A.9})$$

Also

$$\gamma_l^2 = S_l (\gamma_l^{sp})^2 \quad (\text{A.10})$$

is the observable reduced width and S_l is the SF in the single-particle approximation.

Appendix B: Two interfering resonances in R -matrix approach

Here we consider the application of the R -matrix method for two interfering resonances following [17, 18]. The expression of the S -factor for two-level, two-channel case is given by

$$\begin{aligned} S(E)(\text{MeVb}) &= \frac{\hat{J}_R}{\hat{J}_a \hat{J}_A} \lambda_N^2 m_{au}^2 e^{2\pi \eta_i} \frac{2\pi}{\mu_i} 10^{-2} \\ &\times P_f(E_f) P_i(E) \left| \sum_{\nu \tau} \tilde{\gamma}_{f\nu} [\mathcal{A}^{-1}]_{\nu\tau}(E) \tilde{\gamma}_{i\tau} \right|^2, \end{aligned} \quad (\text{B.1})$$

where J_R is the spin of the resonance, J_i is the spin of particle i , $\tilde{J}_i = 2J_i + 1$, λ_N is the Compton wavelength, m_{au} is the atomic mass unit, μ_i and η_i are the reduced mass and the Coulomb parameter of the particles a and A in the initial channel, P_i and P_f are the penetrability factors in the channels i and f , $\tilde{\gamma}_{c\nu}$ is the formal reduced width amplitude in the channel $c = i, f$ and level $\nu = 1, 2$. E_c is the relative kinetic energy of the particles in channel c and $E \equiv E_i$. We assume that the SFs for levels $\nu = 1, 2$ are equal to unity. The level matrix in the

R -matrix method is defined as

$$[\mathcal{A}]_{\nu\tau}(E) = (E_\nu - E) \delta_{\nu\tau} - \sum_{c=i,f} \tilde{\gamma}_{c\nu} \tilde{\gamma}_{c\tau} [\hat{S}_c(E_c) - B_c + iP_c]. \quad (\text{B.2})$$

Here $\hat{S}_c(E_c)$ is the energy shift in the channel $c = i, f$ (see Eq. (A.5)), and B_c is the level-independent boundary condition in the channel c and E_ν is the eigenenergy of level $\nu = 1, 2$, which is the R -matrix fitting parameter.

In the fit it is convenient to take one of the level eigenenergies equal to the resonance energy of the corresponding level, for example $E_1 = E_{R_1}$ and $B_c = \hat{S}_c(E_{R_1})$. E_{R_1} is the real part of the resonance energy of the level 1. Then the second eigenvalue E_2 is the fitting parameter, which deviates from the resonance energy E_{R_2} of the second level. After that, using the Barker's transformation [17] one can find the energy of the second resonance.

-
- [1] J. H. Kelley *et al.*, Nucl. Phys. A, **880**, 88 (2012).
[2] B. Vande Kolk *et al.*, Phys. Rev. C **105**, 055802 (2022).
[3] A. Cvetinović *et al.*, Phys. Rev. C **97**, 065801 (2018).
[4] J. Okołowicz, M. Płoszajczak, and W. Nazarewicz, Phys. Rev. C **107**, L021305 (2023).
[5] A. M. Boesgaard, C. P. Deliyannis, and A. Steinhauer, Astrophys. J. **621**, 991 (2005).
[6] C. Angulo *et al.*, Z. Phys. A **345**, 333 (1993).
[7] C. Spitaleri *et al.*, Phys. Rev. C **90**, 035801 (2014).
[8] C. Spitaleri *et al.*, Phys. Rev. C **95**, 035801 (2017).
[9] A. M. Mukhamedzhanov, Eur. Phys. J. A (2023).
[10] N. K. Timofeyuk, R. C. Johnson, and A. M. Mukhamedzhanov, Phys. Rev. Lett. **91**, 232501 (2003).
[11] A. M. Mukhamedzhanov, Phys. Rev. C **99**, 024311 (2019).
[12] A. M. Mukhamedzhanov and L. D. Blokhintsev, Eur. Phys. J. A **58**, 29 (2022).
[13] R. J. Furnstahl and H.-W. Hammer, Phys. Lett. B **531**, 203 (2002).
[14] A. M. Mukhamedzhanov and A. S. Kadyrov, Phys. Rev. C **82**, 051601(R) (2010).
[15] S. Hinds and R. Middleton, Nucl. Phys. **38**, 114 (1962).
[16] H. T. Fortune *et al.*, Phys. Rev. C **7**, 136 (1973).
[17] F. C. Barker, Aust. J. Phys. **25**, 341 (1972).
[18] F. C. Barker, Phys. Rev. C **78**, 044611 (2008).